Bevel or Not: Identifying the Potential of Bevels for Touch Input Accuracy on Ring Device

Yuki Kubo
NTT Human Informatics Laboratories
NTT, Inc.
Yokosuka, Kanagawa, Japan
yuki.kubo@ntt.com

Arinobu Niijima
NTT Human Informatics Laboratories
NTT, Inc.
Yokosuka, Kanagawa, Japan
arinobu.niijima@ntt.com

Yukio Koike
NTT Human Informatics Laboratories
NTT, Inc.
Yokosuka, Kanagawa, Japan
yukio.koike@ntt.com

Buntarou Shizuki
IPLAB
University of Tsukuba
Tsukuba, Ibaraki, Japan
shizuki@cs.tsukuba.ac.jp

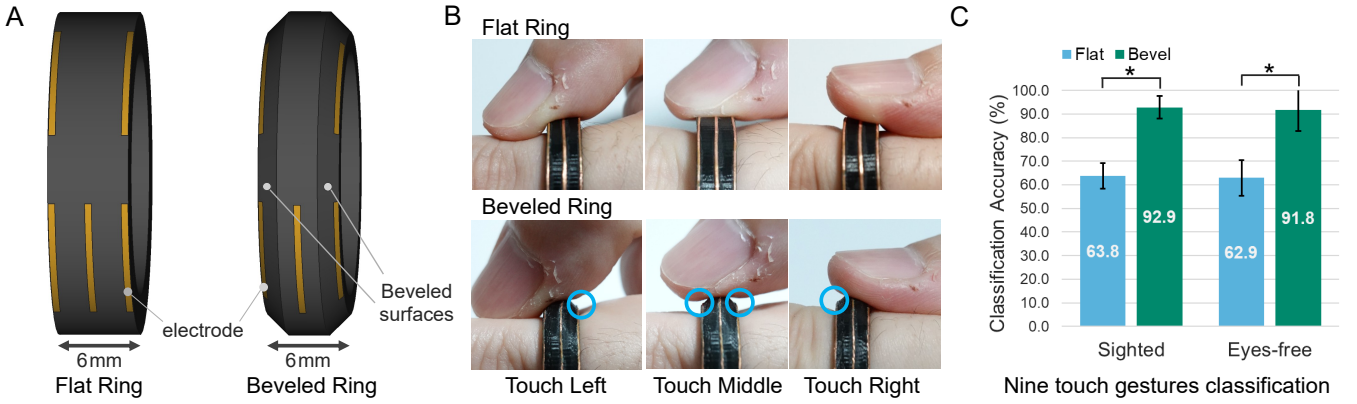


Figure 1: Overview of our method. A) We investigate the effectiveness of beveled surfaces as an input surface in addition to the flat outer surface. B) Differences in surface angles create tiny gaps between the finger pad and non-target surfaces at contact, reducing accidental touch inputs. Even narrow rings enable expressive, accurate input. C) Study 2 evaluation of nine touch gesture classes shows that Beveled Ring with 6 mm band width has significantly higher accuracy than Flat Ring, under both sighted and eyes-free conditions.

Abstract

Smart rings can serve as a wearable platform for off-device control of nearby devices. However, their thin bands lead to a small touch surface on the ring, limiting touch input expressivity and accuracy. To address this, we investigate the effectiveness of ring shapes that use beveled surfaces in addition to the flat outer surface as input surfaces. The distinct angles of the three surfaces limit touches to the intended surfaces, improving accuracy. A first study showed that with band widths of 6 mm or less, flat rings achieved low accuracy (63.8%) in distinguishing between left and right edge touches, whereas beveled and rounded rings achieved high accuracy (90.0%, 93.3%). In a second study of nine touch gestures on 6-mm rings, beveled rings outperformed the flat rings, achieving 92.9% (sighted) and 91.8% (eyes-free) with FPR ≤ 1%. Through these investigations, we identify beveled surfaces as a promising method toward expressive, precise touch input.

CCS Concepts

• **Human-centered computing** → **Human computer interaction (HCI)**; **Touch screens**; **Gestural input**; *Interaction devices.*

Keywords

Touch input, Ring shape design, Edge interaction, Beveled surfaces, Smart ring.

This work is licensed under a Creative Commons Attribution 4.0 International License.

CHI '26, Barcelona, Spain

© 2026 Copyright held by the owner/author(s).

ACM ISBN 979-8-4007-2278-3/26/04
https://doi.org/10.1145/3772318.3790637

ACM Reference Format:
Yuki Kubo, Arinobu Niijima, Yukio Koike, and Buntarou Shizuki. 2026. Bevel or Not: Identifying the Potential of Bevels for Touch Input Accuracy on Ring Device. In *Proceedings of the 2026 CHI Conference on Human Factors in Computing Systems (CHI '26), April 13–17, 2026, Barcelona, Spain.* ACM, New York, NY, USA, 15 pages. https://doi.org/10.1145/3772318.3790637

1 Introduction

Smart rings are finger-worn wearable devices that embed sensing and computational functions into a ring-shaped form factor. They have been explored for applications such as health monitoring and contactless payment [21, 27]. By leveraging a compact and unobtrusive form factor, smart rings provide an alternative platform for everyday interaction with digital systems [1, 7]. For example, some studies have explored functions such as non-invasive health monitoring of physiological indicators [21, 28, 63], contactless payment [27, 48, 49], control of other wearables [47], and interaction with nearby environmental smart devices [1, 7]. We believe that next-generation smart rings have the potential to evolve into general-purpose smart devices that support various daily tasks with the integration of these functions.

Although these scenarios, such as off-device control of nearby devices, are highly appealing, operating smart rings presents distinct challenges as touch input devices, due to their compact size, lack of graphical displays, and frequent use without visual attention (i.e., eyes-free). The number of physical touch areas or buttons that can be placed on a ring is limited (typically one to four) [32, 47], which constrains interaction and often requires multi-step operations for device control [22]. One study on the preferred numbers of gestures suggests that systems offering around five to nine distinct gestures are most favored over those with fewer than five or more than ten [13]. Additionally, gesture sets within that range have been proposed based on user studies [11, 19, 55]. In order to expand the range of applications for the device, researchers are exploring interaction techniques and scenarios for ring devices [7, 18]. For example, ParaGlassMenu [7] examined a finger-worn device with four buttons and a touchpad for operating optical HMDs, while ThumbText [18] proposed a ring-mounted touchpad for thumb-based text entry. These devices provide stable touch input by using larger touch areas and buttons, which compromise both wearability and aesthetics. Given that ring devices are worn daily as jewelry, functionality (e.g., device control) must be balanced against comfortable, discreet form factors appropriate for everyday wear [23, 30, 38, 39]. We argue that for smart rings to be widely adopted as always-worn devices, it is essential to develop methods that enhance the expressiveness and accuracy of input while maintaining their compactness and wearability.

An alternative method in this field is to use edge touches, where input is performed on the device's physical edges or bezels. Prior work on edge and bezel-based interactions has been proposed in several devices, such as portable devices [34, 58], tablets [50], smartphones [15, 42], and smartwatches [20, 59]. Even with a limited surface area, edge input can provide an accessible and low-error method of interaction. Ring devices have two edges that the thumb can easily reach, and this characteristic could potentially enhance both the expressiveness and accuracy of input. At the same time, ring band widths are often narrower than the touch-target sizes recommended by fat-finger studies [37]. This raises concerns that relying on edge cues alone may be insufficient to prevent accidental touches. Moreover, while some commercial smart rings have a band width of 7.9 mm (Oura Ring 4 [26]), there are also products with band widths of 7.0 mm (Galaxy Ring [46]) and 6.8 mm (RingConn Gen 2 [41]). Similar to the variety in smartphone size, future smart ring designs may explore a variety of band widths, including narrower ones, for wearability and aesthetic reasons. In such cases, the reduced surface area may further increase the risk of erroneous input. Previous fat-finger studies have primarily examined flat displays larger than the fingertip, raising the question of whether the same issues also occur in edge touches on the narrow form factor of rings. To address this gap, we conduct the first systematic investigation of fat-finger problems in edge touch input on a ring device across different ring band widths. Our study offers initial insights and design implications for improving input accuracy while maintaining the wearability and aesthetics of rings. We argue that further design explorations and systematic evaluations of edge-touch input techniques are indispensable for advancing smart ring input capabilities.

To improve the precision of edge touches on rings, we investigate the feasibility of using beveled surfaces, in addition to the flat outer surface, as input surfaces. The angled three-surface arrangement may allow users to tilt the finger for clearer touch separation without conscious effort, while the differing surface orientations may help reduce accidental contacts, potentially improving input accuracy. Several studies have explored the use of shape design to improve input usability [5, 34, 44]. Prior work leveraging angled surfaces has demonstrated their effectiveness in enhancing input accuracy, highlighting the simplicity, versatility, and refinement of using beveled surfaces. These insights underscore the suitability of such approaches for small wearable devices, where design and wearability are essential attributes. Despite the promise of the use of beveled surfaces for touch input, no prior work has systematically investigated edge touch input on rings. This paper addresses this gap by presenting the first design, implementation, and evaluation of edge touch input on a ring device, and demonstrates that beveled surfaces are promising for achieving expressive and precise touch input while preserving wearability.

In this paper, we evaluate the feasibility of using beveled surfaces, in addition to the flat outer surface, for touch input on rings through two studies (Figure 1). These studies investigate the necessity and effectiveness of beveled surfaces for edge touch input. First, we evaluate whether users can accurately input on the left surface, right surface, and flat middle surface across three band widths (4 mm, 6 mm, and 8 mm) and three ring shapes: Flat, Beveled, and Rounded. The results show that when the band width is 6 mm or less, distinguishing between the left and right edges becomes difficult on Flat Ring, whereas Beveled and Rounded Rings significantly improve surface targeting accuracy (i.e., the accuracy of touches on the intended input surfaces). Whereas edge touches on Flat Ring are susceptible to errors caused by fat-finger effects under certain conditions, our results suggest that introducing ring shape design can significantly improve input accuracy. Second, we compare the classification accuracy of nine touch gestures (Figure 2) on Flat and Beveled Rings with 6 mm band width under both sighted and eyes-free conditions. The results show that, under both conditions, Beveled Ring enables users to perform touch gestures with significantly higher accuracy and lower false positive rates than Flat Ring. By enabling a more precise set of touch inputs, our work identifies the potential of beveled surfaces in supporting advanced interaction scenarios for smart rings. The contributions of this paper are as follows:

- We identify beveled surfaces as a promising method toward expressive and precise touch input on a ring device through two investigations. The results offer valuable insights for future research, allowing designers and researchers to build upon and expand ring input applications.
- We conduct the first systematic investigation into whether fat-finger effects occur in edge touch input across different ring band widths and ring shapes. The results suggest that when the band width is 6 mm or less, distinguishing left and right edge touches becomes difficult on Flat Ring due to the fat-finger effects. Beveled and Rounded Rings can significantly improve the surface targeting accuracy over Flat Ring at these band widths.
- We conduct a user study to evaluate the classification accuracy of nine touch gestures for Flat and Beveled Rings with 6 mm band width under sighted and eyes-free conditions. The results show that Beveled Ring outperforms Flat Ring in both classification accuracy and FPRs, achieving 92.9% and 91.8% accuracy in the sighted and eyes-free conditions, respectively, with FPR $\leq$ 1% (0.88% sighted; 1.00% eyes-free).

2 Related Work

2.1 Interaction on Ring Devices

Smart rings have become increasingly popular due to their health monitoring capabilities, and ring devices equipped with advanced computational resources are now appearing more frequently in daily use [26, 41, 46]. Researchers have explored a variety of functions for such devices, including health monitoring [21, 62, 63], contactless payment [27, 48, 49], control of other wearable devices [47], and interaction with nearby environmental smart devices [1, 7]. These studies conceptualize ring devices as multipurpose devices that support users in various everyday tasks. To accommodate such various functionalities, several studies have proposed touch interaction techniques for ring devices [1, 7, 18, 32, 47]. Touch input has been highlighted as a promising technique, as it is familiar to users through widespread smartphone interaction, offers the convenience of one-thumb operation, and provides tactile feedback. For example, EyeRing [32] is a finger-worn camera device for assisting visually impaired users, where a touch button is used to trigger image capture and recognition. Sapkota et al. [47] explored heads-up interactions with a ring-type device that allows users to control nearby wearable devices using touch input on four physical buttons. This limited number of buttons constrains interaction, and multiple steps may be needed to control a target device. In addition, prior work has explored interaction techniques and scenarios for ring devices. For example, ParaGlassMenu [7] examined a finger-worn device for optical HMD menu operations; it featured a 33 mm diameter touch area on top of the ring, with four buttons and a touchpad. ThumbText [18] mounted a 13 mm $\times$ 18 mm touchpad with six regions on a ring to enable thumb-based text entry. These devices provide stable touch input by using larger touch areas and buttons, which compromise both wearability and aesthetics. Given that ring devices are worn daily as jewelry, functionality (e.g., device control) must be balanced with comfortable, discreet form factors appropriate for everyday wear [23, 30, 38, 39]. Building on this line of work, our method seeks to realize expressive and precise touch input by beveling the ring surface to enable clearer separation between touch surfaces, while preserving wearability.

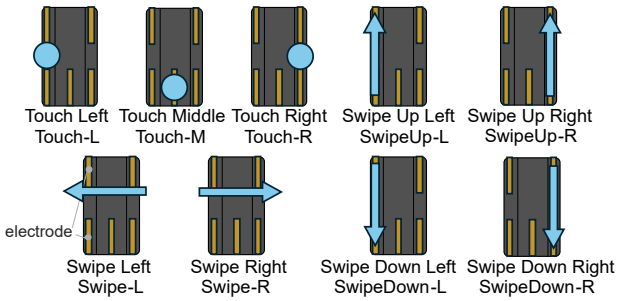


Figure 2: Nine touch gestures using three input surfaces: left and right beveled surfaces and flat middle surface. These gestures consist of three Touch gestures, Four Swipe Up and Down gestures, and two Swipe gestures. These gestures are classified based on the five electrodes and their temporal order of interaction.

2.2 Touch Interaction on Small Devices

Although touch devices offer portability and wearability, they are inherently limited by their small input surface area. To address this, researchers have investigated ways to enhance the expressiveness and accuracy of touch interaction. One approach has been to explore using surfaces beyond the front display plane to enable more precise touch input on small devices. Specifically, researchers have proposed using the back [4, 57], the sides [24, 25, 36], and even the hover space above the device [9, 12] as additional input areas. These studies collectively demonstrate that using non-planar or off-screen surfaces can improve usability and expand the interaction possibilities.

Another line of work has focused on touch input on the display plane itself. One of these approaches involves leveraging the device's physical edges or bezel as input surfaces. Prior work on edge and bezel-based interactions has been proposed in several devices, such as portable devices [34, 58], tablets [50], smartphones [15, 42], and smartwatches [20, 59]. These studies demonstrated that the screen's edges can serve as tactile landmarks, supporting stable and precise touch inputs along their edges. Even with a limited surface area, using the edges for touch input can provide an accessible and precise method of interaction. Ring devices have two edges that the thumb can easily reach, and this characteristic could potentially enhance both the expressiveness and accuracy of input.

In band widths suitable for everyday wear [6, 26], rings are often narrower than the target sizes recommended in fat-finger studies [37], raising concerns that relying solely on edges may not prevent mistouches. The fat-finger problem [51] refers to the phenomenon in which the finger pad spreads upon contact, causing error rates to increase as target size decreases. Parhi et al. [37] reported that errors increase when targets are smaller than 9.6 mm for discrete tasks and 7.7 mm for continuous tasks. In our method, we use beveled surfaces and define three input surfaces on its outer band: the left surface, the flat middle surface, and the right surface. If the band width is 8 mm and these three surfaces are simply divided

equally, each surface would be only about 2.6 mm wide, which is less than half of the recommended target size. This motivated our investigation into what band width allows precise three-region discrimination without incurring fat-finger errors. Such insights can provide valuable design insights for edge-based touch input for smart rings. We also investigated whether different ring geometries, such as beveled surfaces, can improve the accuracy of edge-touch input.

2.3 Shape Design for Input Interfaces

Functional input interfaces that leverage shape design have been explored across a wide range of domains, including desktop devices [44, 53] and mobile and wearables devices [34]. Furthermore, applications have also been explored in specific contexts, such as everyday material interfaces [14, 33], in-vehicle control panels [5], and accessibility support [16, 58]. The physical shape guides and supports hand and finger movements, enhancing usability with less conscious effort from the user. Ergonomic considerations, such as angles, curvature, and surface friction, have been examined to provide a comfortable user experience and improved functionality. The usability of input interfaces, such as ergonomically informed studies, has been evaluated in the HCI field [2, 29, 56]. Moreover, leveraging physical form instead of computational resources allows these approaches to remain simple and to be implemented without imposing additional processing overhead. For example, Roudaut et al. [44] developed a touch device with convex and concave surfaces and investigated how surface curvature affects finger posture and, consequently, input accuracy. Bhaumik et al. [5] designed console prototypes with the front face angled at 45°, 90°, and 135° and evaluated through user studies how these geometries alter hand posture, thereby influencing input accuracy. Interaction on the Edge [34] uses the perpendicular edge of a small device's screen as an input surface, enabling occlusion-free and precise touch interaction. These studies show that physical geometry and orientation can guide hand and finger posture, thereby influencing touch input accuracy. Building on these insights, our work evaluates the use of a beveled surface on a ring device to guide finger contact during touch interaction; we aim to improve input accuracy while preserving both wearability and aesthetics.

3 Research Question

We investigate the potential of using beveled surfaces to augment a flat outer surface, aiming for more expressive and accurate touch input on a ring device (Figure 3A). The research question presented in this paper is as follows:

RQ: How do beveled surfaces affect touch input on a ring device?

This research question is grounded in a simple observation: beveled surfaces induce an upward finger pitch (i.e., tilt) on edge touch, which induces a small gap between the ring's surfaces and the fingerpad (Figure 3B). This subtle change may allow users to touch the intended surface without accidentally contacting others, even with a narrower ring. Specifically, we compare Flat and Beveled Rings on narrow rings and quantify input accuracy. The observation suggests that beveled surfaces may enhance not only accuracy but also the expressiveness of touch input on rings, by

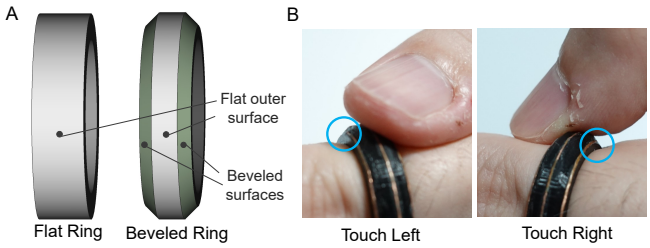


Figure 3: Example ring shape. A) Flat Ring has only a flat outer surface and no edge surfaces. Beveled Ring has beveled surfaces that can be used as input surfaces, as well as a flat outer surface. B) Differences in surface angles create tiny gaps between the finger pad and non-target surfaces at contact in Beveled Ring, reducing accidental touches.

enabling users to distinguish and selectively use three input surfaces, including the beveled surfaces. We investigate the feasibility of using beveled surfaces to identify their potential for enabling precise and expressive touch input on ring devices.

If beveled surfaces are effective for touch input, our method may offer several features. First, because its passive ring shape requires no additional computation, resulting in virtually no additional latency or power consumption. Second, touch detection and gesture classification do not require machine learning, so training data is not necessary. Third, the design can be implemented in a compact ring shape, improving functionality while preserving wearability.

4 Experimental Device and System

We built an experimental ring device and system to investigate how ring shape affected touch input accuracy. The setup consisted of the ring device, a touch sensing circuit, and a microcontroller.

4.1 Ring Devices

To evaluate touch input accuracy on a compact ring shape, we 3D-printed the ring body and attached electrodes to three input surfaces on the ring. The resulting ring device detects touch and serves as our evaluation ring.

We designed the ring bodies in 3D CAD and fabricated them using a 3D printer. For evaluation, we prepared three ring shape variants: a flat ring with no edge facet (Flat Ring), a ring with two 45° edge chamfers (Beveled Ring), and a ring with an elliptical (rounded) edge chamfer (Rounded Ring). The models were printed on an Ultimaker S5 using TPU 95A filament. To accommodate individual differences in finger diameter, the lower portion of the ring uses an open-ended design.

Electrodes made from copper foil tape and a flexible conductive film (approximately 0.5 mm wide) were glued to the ring's surface. We wired each electrode to a capacitive touch sensor module and covered the electrode-contact points with insulating tape.

4.2 Touch Sensing System

The touch sensing system consisted of a capacitive touch sensing module (MPR121, NXP Semiconductors) and a microcontroller (Feather nRF52840 Express, Adafruit Industries, LLC). The module

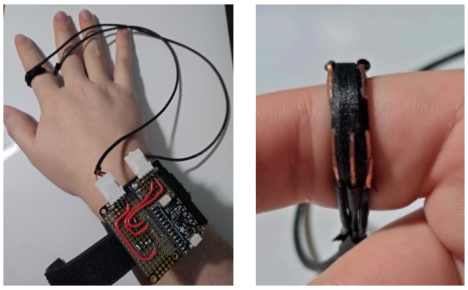


Figure 4: Experimental device setup. The setup consisted of a ring device and an enclosure mounting a capacitive touch sensing module and a microcontroller. The ring was connected to the module by wires.

measured each electrode's capacitance and performed threshold-based touch detection. The measured values were retrieved by the microcontroller over I2C. During the study, the microcontroller was connected to a laptop via a wired serial link, over which touch data were streamed and recorded. These measured values were recorded and analyzed. The touch sensing module was used as an MPR121-based breakout board (ADA-1982, Adafruit Industries, LLC). The microcontroller supports Bluetooth Low Energy (BLE) and battery power, enabling wireless standalone operation.

For the evaluation, the touch sensing module and the microcontroller were mounted in an enclosure as shown in Figure 4 that could be mounted on a wristband. The ring was connected to the module via a wired connector, allowing rings to be swapped quickly so that different ring designs could be evaluated.

5 Study 1: Ring Band Width and Shape Effects on Surface Targeting Accuracy

In this study, we evaluate whether users could accurately perform touch input on the left edge, right edge, and flat outer surface of rings with three band widths (4 mm, 6 mm, and 8 mm) and three ring shapes (flat, beveled, and rounded). The first aim was to evaluate whether different ring shapes enabled users to touch only the intended input surface, that is, to what extent ring shape reduced unintended touches on input surfaces other than the intended one. The second aim was to evaluate whether band widths affect targeting accuracy, which has not been systematically investigated before. We evaluated these effects using the accuracy of touches on the intended input surface (surface targeting accuracy) and the classification accuracy of vertical swipe gestures on the ring devices. This study was conducted with approval from the local Institutional Review Board (IRB).

We collected data on gestures from 15 participants (8 males and 7 females, range: 20s–40s, mean age: 33.2 years, SD = 7.75 years). All participants were right-handed except for one left-handed participant. The mean participant completion time was 86 minutes for all tasks.

5.1 Apparatus

We defined nine ring conditions (Figure 5A) by factorially combining three band widths (4 mm, 6 mm, and 8 mm) and three ring shapes (flat, beveled, and rounded). These conditions were then used to evaluate surface targeting accuracy and classification accuracy on each surface. All rings were 3 mm thick, following a commercial smart ring (Oura Ring 4 [26]; about 2.8 mm). The band width conditions were also determined following Oura Ring 4 (7.9 mm wide). We used 8 mm and, considering the potential miniaturization of smart rings, also included 6 mm and 4 mm. The chamfer angle of Beveled Ring was set to 45°, because 45° is widely used as the standard chamfer angle in machining [8, 31]; we therefore used this angle as the initial choice for our evaluation. The ring shape conditions (Flat, Beveled, Rounded) were as follows:

- **Flat Ring:** A ring whose input surface consists of only a flat outer surface, with no chamfering on either edge. Ring cross-section is rectangular, with a width equal to the band width.
- **Beveled Ring:** A ring with a 1.5 mm, 45° chamfer applied to both edges. This design reduces the width of the flat middle surface to 1 mm, 3 mm, and 5 mm for band widths of 4 mm, 6 mm, and 8 mm, respectively.
- **Rounded Ring:** A ring with both edges rounded. Its cross-section consists of two parts: a rectangular lower section with a height of 1.5 mm, and a semi-elliptical upper section with a height of 1.5 mm and a major axis equal to the band width.

To detect touch input on the left edge, right edge, and flat middle surface, we placed electrodes on each ring condition, as shown in Figure 5B. The electrodes on the left and right edges were placed on the surface of the ring, aligned with the side. This configuration was adopted because if errors occurred under this setup, they would be expected to occur even more frequently with electrodes placed further inward. Touches were detected when a finger made contact with the corresponding electrode. To accommodate variations in participants' finger size, we fabricated the ring-shaped device in four inner diameters (14 mm, 16 mm, 18 mm, and 20 mm).

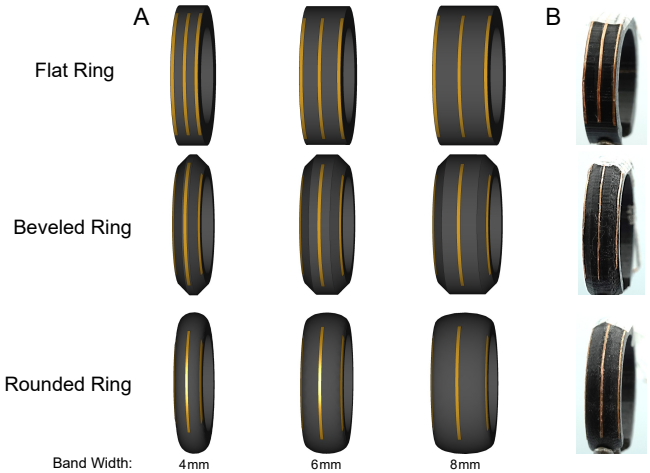


Figure 5: Nine ring conditions in Study 1. A) The nine ring conditions consist of combinations of three band width conditions (4 mm, 6 mm, and 8 mm) and three ring shape conditions (Flat, Beveled, and Rounded). B) Examples of ring devices, each ring shape has a 6 mm band width.

For Study 1, these ring bodies were printed using CPE+ filament, and 36 rings were fabricated in total (4 inner diameters × 9 ring conditions).

Touch detection for the electrodes on the ring device in Study 1 was implemented using the CapSense library [3]. The electrodes were connected to an Arduino Due, and the capacitance of each electrode was measured. The CapSense circuit used a 100 kΩ resistor, and the measured values were transmitted via serial communication at approximately 90 Hz. A touch was detected when the electrode's capacitance exceeded a predefined threshold. In Study 1, we calibrated a touch-detection threshold for each participant before the experimental trials. This calibration controlled for individual differences in capacitance changes (e.g., due to age or dry fingertips), enabling us to evaluate the effect of ring shape on touch input. First, participants were asked to keep their fingers away from the ring while we observed the baseline capacitance values of all electrodes for several seconds. Next, they were instructed to touch each electrode (left, middle, and right) with their fingertip, and we observed the capacitance values during contact. The experimenter then set the threshold so that none of the electrodes exceeded the threshold in the non-contact state, whereas contact with any electrode would cause its capacitance to exceed the threshold. These experimental ring devices were configured so that they would not respond when a finger merely approached an electrode without physically touching it, because the electrode width was only approximately 0.5 mm. In Study 1, CapSense touch thresholds for all participants were set in the range 75–120.

We set a single touch-detection threshold for each participant and applied the same value to all ring shapes (flat, beveled, and rounded), thereby aligning the sensing conditions across shapes. Using this experimental configuration, we compared the different ring shapes under same sensing parameters to evaluate the effect of geometric differences in ring shape on touch input accuracy rather than corrections introduced by threshold adjustments. Before the experimental trials for each ring condition, we confirmed that the chosen threshold enabled touch detection for all ring devices, so that no particular shape suffered from undetected touches or unfair evaluation.

5.2 Tasks

In Study 1, we investigated how ring band width and shape affect input accuracy by asking participants to perform upward and downward swipes (SwipeUp/Down) on three input surfaces of the ring (left, flat middle, and right surfaces), as shown in Figure 6A. Swiping was chosen because tracing each surface from top to bottom leads to variations in the thumb's angle and posture, thus covering a wide range of contact positions on the ring. Swipes on the left or right edge were classified as errors if the finger also touched the opposite edge electrode, but touching the middle surface during these swipes was allowed. For swipes on the middle surface, any contact with one or both edge electrodes was classified as an error. Criterion 1 (C1) was defined to examine whether users can intentionally distinguish and touch each of the three input surfaces on the ring, as shown in Figure 6B.

Participants were instructed to perform SwipeUp/Down gestures (Figure 6A) on three input surfaces of the ring (left edge, right edge, and flat middle surface), under nine ring conditions. Each participant completed ten sessions for each condition. In each session, they performed the six gestures once in a randomized order. The order in which the rings were worn was also randomized across the nine conditions to avoid order effects. In total, we collected 8,100 gesture trials (15 participants × 9 conditions × 10 sessions × 6 gestures).

5.3 Procedure

Participants first sat in front of a display that presented on-screen task instructions. To determine the appropriate ring size, participants measured the length and width of their fingers and selected one from four options. Participants then attached the ring to the proximal phalanx of the index finger of their dominant hand. After this, participants then read a document detailing the experimental procedures and the six gestures. In this document, participants were asked to perform each gesture as accurately as possible.

Before the experimental sessions, participants practiced each gesture while observing real-time sensor values from the electrodes displayed as bar graphs. A touch detection threshold was set individually for each participant. After this practice phase, participants were asked to conduct the experimental sessions, performing the six gestures in randomized order while following on-screen instructions, with a 0.5-second interval between trials. Participants were also asked to report any errors (e.g., performing a gesture different from the on-screen instruction). When an error trial was reported, the corresponding trial was performed again according to the on-screen instructions, and the data for that trial were recollected. After completing a set of experimental sessions for one ring, participants removed it, wore the next one, and repeated the procedure until all ring conditions were completed. Participants were provided with at least a one-minute break between rings to minimize fatigue.

5.4 Results

To evaluate the effect of bandwidth and ring shapes, we analyzed surface targeting accuracy and classification accuracy of the SwipeUp and SwipeDown gestures on each surface under the nine ring conditions. Error trials were excluded from the analysis, and the recollected trial data were used.

For significance testing of accuracy values, we treated participants as a random factor and ring shape, band width, and swipe direction condition as within-participant factors. Because the assumptions of normality and homogeneity were not satisfied, we conducted a three-factor generalized linear mixed model (GLMM)

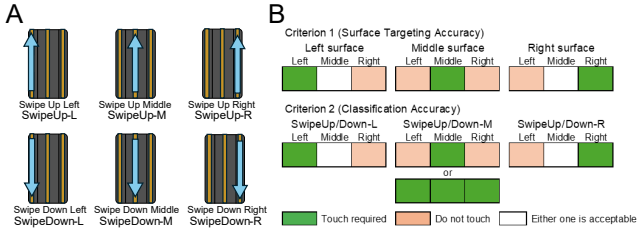


Figure 6: Six swipe gestures used in Study 1 and the criteria for judging each gesture as successful.

with a binomial model on the number of successful trial counts per participant and condition, using the R package lme4. Post-hoc pairwise comparisons were then performed using the emmeans package with Bonferroni-adjusted p-values.

5.4.1 Surface Targeting Accuracy. To evaluate whether users could accurately touch only the intended surface and how ring shape and band width affected this performance, we analyzed surface targeting accuracy for the SwipeUp and SwipeDown gestures on each surface under the nine ring conditions, based on the C1 criterion (Figure 6B). Figure 7 and Table 1 show the mean surface targeting accuracy across participants for swipes on the left, middle, and right surfaces. Figure 8 shows the confusion matrix of surface targeting accuracy.

For the left surface, there were significant main effects of band width ($\chi^2(2) = 39.46$, $p < .001$), ring shape ($\chi^2(2) = 51.34$, $p < .001$), and swipe direction ($\chi^2(1) = 6.85$, $p = .009 < .01$) on surface targeting accuracy. There were also significant interactions between ring shape and band width ($\chi^2(4) = 67.98$, $p < .001$), between ring shape and swipe direction ($\chi^2(2) = 15.29$, $p < .001$), and a significant three-way interaction among ring shape, band width, and swipe direction ($\chi^2(4) = 22.91$, $p < .001$). In contrast, no significant interaction between band width and swipe direction was found ($\chi^2(2) = 5.33, p = .070$). Post-hoc pairwise comparisons showed that, under the 4 mm and 6 mm conditions, both Beveled and Rounded Rings yielded significantly higher surface targeting accuracy than Flat Ring (all comparisons: $adj.p < .0001$). In contrast, at 8 mm there were no significant differences in surface targeting accuracy among the three ring shapes (all $adj.p = 1.00$). Within the Flat Ring conditions, 4 mm and 6 mm rings had significantly lower surface targeting accuracy than 8 mm ([w4-w8], [w6-w8]: $adj.p < .0001$), whereas 4 mm and 6 mm rings showed no significant difference in accuracy ([w4-w6]: $adj.p = 1.00$). Within the Beveled Ring conditions, there was no difference in surface targeting accuracy across the three band widths (all $adj.p = 1.00$). Within the Rounded Ring conditions, 4 mm ring yielded significantly lower surface targeting accuracy than 6 mm ($adj.p < .0001$), while 8 mm ring showed no significant differences (all $adj.p \geq .11$).

For the middle surfaces, only the ring shape showed a significant main effect on the number of successful inputs ($\chi^2(2) = 49.85$, $p < .001$). Neither band width nor swipe direction had a significant main effect (band width: $\chi^2(2) = 0.00$, $p = .999$; swipe direction: $\chi^2(1) = 0.00$, $p = 1.00$). There was a significant interaction effect between ring shape and band width ($\chi^2(4) = 12.98$, $p = .011$), but no significant interaction effects involving swipe direction were found (all $\chi^2 \leq 7.83$, all $p \geq .070$). Flat Ring under the 4 mm and 6 mm band width conditions yielded 0% successful inputs across all trials (floor effect). Because these conditions yielded virtually no variance in performance, they were excluded from the post-hoc multiple comparisons. Pairwise comparisons showed that, across all three widths (4 mm, 6 mm, and 8 mm), Beveled Ring had significantly higher surface targeting accuracy than Rounded Ring (all comparisons: $adj.p < .0001$). Moreover, under the 8 mm condition, Beveled and Rounded Rings showed significantly higher surface targeting accuracy than Flat Ring (all comparisons: $adj.p < .0001$).

For the right surface, both ring shape ($\chi^2(2) = 48.08$, $p < .001$) and band width ($\chi^2(2) = 32.93$, $p < .001$) showed significant main effects, whereas swipe direction did not ($\chi^2(1) = 0.07$, $p = .79$). No significant interaction effects were observed among ring shape, band width, and swipe direction (all $\chi^2 \leq 6.57$, all $p \geq .16$). Pairwise comparisons showed that, under the 4 mm and 6 mm conditions, Beveled and Rounded Rings achieved significantly higher surface targeting accuracy than Flat Ring (all comparisons: $adj.p < .0001$). In addition, within the Flat Ring conditions, 4 mm and 6 mm widths yielded significantly lower surface targeting accuracy than the 8 mm width ([w4-w6], [w4-w8]: $adj.p < .0001$).

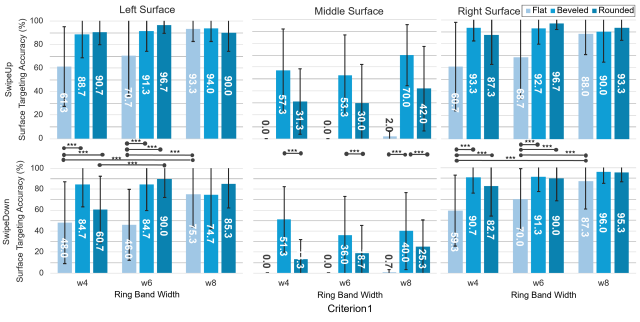


Figure 7: Surface targeting accuracies for left and right surface, and middle surfaces for each band width and ring shape condition. Each bar represents ± one SD between participants.

5.4.2 Classification Accuracy. To evaluate the effects of ring shape and band width on how accurately swipe gestures performed on each input surface could be distinguished, we analyzed the classification accuracy under the nine ring conditions. For the Flat Ring, swipes on the flat middle surface often resulted in contact with all electrodes. This would have yielded low surface targeting accuracy if only C1 was used. To more fairly evaluate classification accuracy among ring shapes, we introduced Criterion 2 (C2), in which swipes that touch all electrodes are classified as valid SwipeUp/Down-M (Figure 6B). Based on C2, we evaluated the number of vertical swipe gestures that could be performed accurately for each ring condition.

Figure 9 shows the mean classification accuracy across participants under C2 for swipes on each surface. The only difference between C1 and C2 is that C2 additionally includes the all-electrode touch pattern; consequently, the mean accuracy changed only for SwipeUp/Down-M (Figure 8). Table 1 shows the C1 results and additionally lists the corresponding C2 values only for SwipeUp/Down-M; SwipeUp/Down-L and SwipeUp/Down-R were unchanged. Figure 8 shows the confusion matrix of classification accuracy. Therefore, we report statistical test results only for the SwipeUp/Down-M classification accuracy under C2.

For SwipeUp/Down-M, there were significant main effects of ring shape ($\chi^2(2) = 81.50$, $p < .001$) and band width ($\chi^2(2) = 7.16$, $p = .028 < .05$) on classification accuracy, whereas swipe direction showed no significant main effect ($\chi^2(1) = 0.94$, $p = .33$). There was also a significant interaction between ring shape and swipe direction ($\chi^2(2) = 11.67$, $p = .003 < .01$). In contrast, no significant interaction effects between ring shape and band width, between band width and swipe direction, or for the three-way interaction among ring shape, band width, and swipe direction were found (all

Table 1: Surface targeting accuracy and classification accuracy (mean ± SD, %) for swipe gestures. Within each surface condition, values are ordered as Flat, Beveled, and Rounded Rings. Criterion 2 differs from Criterion 1 only for the middle surface; therefore, Left/Right are reported once (C1=C2).

		Left (C1=C2)			Middle (C1)			Middle (C2)			Right (C1=C2)		
Gesture	Band	Flat	Beveled	Rounded	Flat	Beveled	Rounded	Flat	Beveled	Rounded	Flat	Beveled	Rounded
SwipeUp	w8	93.3±10.5	94.0±11.2	90.0±15.6	2.0±4.1	70.0±25.6	42.0±35.5	72.0±26.8	72.0±24.3	58.7±31.4	88.0±17.0	90.0±25.6	93.3±10.5
	w6	70.7±34.5	91.3±16.9	96.7±7.2	0.0±0.0	53.3±33.5	30.0±32.3	77.3±27.1	58.0±29.6	51.3±31.4	68.7±34.8	92.7±13.3	96.7±4.9
	w4	61.3±34.0	88.7±20.0	90.7±11.0	0.0±0.0	57.3±34.7	31.3±27.5	82.0±23.1	59.3±34.7	56.0±26.9	60.7±36.9	93.3±11.1	87.3±24.6
SwipeDown	w8	75.3±31.6	74.7±32.3	85.3±23.3	0.7±2.6	40.0±36.8	25.3±25.6	75.3±29.5	42.0±35.3	33.3±25.8	87.3±26.3	96.0±10.6	95.3±8.3
	w6	46.0±33.8	84.7±25.3	90.0±18.1	0.0±0.0	36.0±37.0	18.7±26.7	84.7±22.9	40.0±33.8	34.0±29.5	70.0±29.0	91.3±14.1	90.0±21.4
	w4	48.0±39.0	84.7±21.7	60.7±31.7	0.0±0.0	51.3±31.4	13.3±18.4	86.0±16.4	53.3±31.1	32.7±26.0	59.3±33.7	90.7±14.9	82.7±28.6

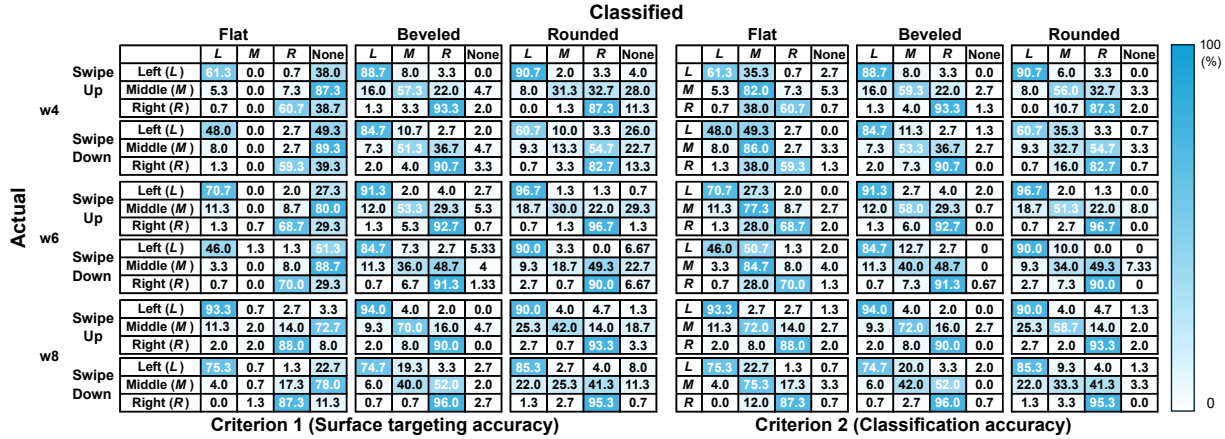


Figure 8: Confusion matrices for surface targeting accuracy and classification accuracy.

$\chi^2 \leq 7.81$, all $p \geq .099$). Post-hoc pairwise comparisons showed that, across all three band widths (4 mm, 6 mm, and 8 mm), Flat Ring had significantly higher classification accuracy than Beveled and Rounded Rings ([w8, Flat-Beveled]: $adj.p = .0011 < .01$, other comparisons: $adj.p < .0001$). Within each ring shape (Flat, Beveled, and Rounded), there were no significant differences in accuracy among the three band widths (all $adj.p > .05$).

5.4.3 Discussion. Under C1, left and right surfaces at 4 mm and 6 mm in Flat Ring condition had significantly lower surface targeting accuracy than at 8 mm. As shown in Figure 8, many error trials labeled None under C1 are instead classified as Middle under C2, indicating that these errors occurred when the thumb contacted all electrodes simultaneously, see Figure 6B. In other words, these results suggest that, when the band width is small, a surface targeting on either edge can cause the thumb pad to span the entire flat outer surface of the ring. Therefore, when the band width is 6 mm or less, distinguishing left and right surface touches becomes difficult on Flat Ring due to fat-finger effects. For the smaller band widths (4 mm and 6 mm), surface targeting accuracy on the left and right surfaces was significantly higher in Beveled and Rounded Rings than in Flat Ring. These results suggest that ring shape design choices, such as Beveled and Rounded Rings, improve surface targeting accuracy with narrow widths.

For the middle surface under C1, Beveled Ring achieved a significantly higher accuracy than Rounded Ring. For Flat Ring, the middle surface yielded accuracy of nearly 0%. These error trials that were labeled as None under C1 are instead classified as Middle under C2, indicating that these errors are caused not by touching either the left or right edges alone but by simultaneous contact with both edge electrodes, as shown in Figure 8. Rounded Ring also showed that trials labeled as None under C1 were instead classified as Middle under C2. Moreover, Rounded Ring with band width of 4 mm had significantly lower accuracy on the left surface than that with band width of 6 mm. These results show that Rounded Ring causes more frequent unintended touch of both edge electrodes, resulting in lower surface targeting accuracy than Beveled Ring. These results suggest that, under our experimental setup, Beveled Ring enables users to accurately and selectively touch only the intended surface significantly more often than Rounded Ring.

The classification accuracy results for SwipeUp/Down-L and SwipeUp/Down-R were the same as the surface targeting accuracy results. That is, under the band width of 4 mm and 6 mm, Beveled and Rounded Rings allow users to perform two vertical swipes accurately on the left and right surfaces than Flat Ring. In contrast, for SwipeUp/Down-M, Flat Ring enabled significantly more accurate swipes than the other ring shapes. On the other hand, under the 8 mm band width, the mean accuracy of SwipeUp/Down-M is 73.7%, which is still lower than the accuracies achieved on the left and right surfaces (84.3% and 87.7%). Although there were no significant differences among band widths, Flat Ring showed a tendency for mean accuracy to increase as the band width decreased (84.0%,

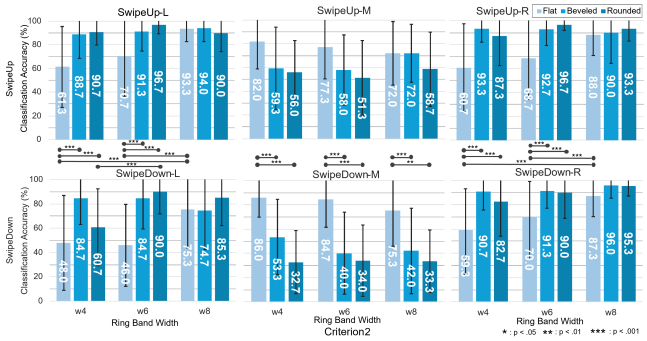


Figure 9: Mean classification accuracies for SwipeUp/Down gestures on left, middle, right surfaces for each band width and ring shape condition. Each bar means ± one SD between participants.

81.0%, and 73.7% for 4, 6, and 8 mm, respectively). These results may be due to the fact that narrower bands make it easier for the thumb to contact all electrodes in Flat Ring.

In summary, under our experimental setup, all three ring shapes with 8 mm band width could accurately support two vertical swipes. At 4 mm and 6 mm band widths, Flat Ring allowed users to perform one vertical swipe accurately, those on the middle surface (SwipeUp/Down-M). Beveled and Rounded Rings allowed users to perform two vertical swipes accurately on the left and right surfaces (SwipeUp/Down-L and SwipeUp/Down-R). Of particular interest, the Rounded Ring showed significantly lower SwipeUp/Down-L accuracy at 4 mm band width than at 6 mm. Based on the surface targeting accuracy results, Flat Ring made it difficult to touch only the middle surface. Beveled Ring had a significantly higher surface targeting accuracy for the middle surface than Rounded Ring. These results suggest that, within our study conditions, the beveled surface may best attain intended surface touches. Our results suggest that ring shape design influences touch input accuracy on ring devices and may improve it.

6 Study 2: Beveled Surface and Touch Gesture Classification Performance

Building on the results from Study 1, we next investigated whether the beveled surface design improves the accuracy of touch gestures. Specifically, the aim is to examine whether the beveled surface reduces misclassification of touch gestures and improves input accuracy. To evaluate this, we conducted an experiment using two 6 mm-wide ring devices: a Flat Ring and a Beveled Ring. Participants were asked to perform nine touch gestures on these rings (Figure 2), and we compared the classification accuracy and false-positive rate (FPR) for these gestures for the two ring shapes. This study was approved by the local IRB.

We collected gesture data from 12 participants who did not participate in our first study (7 males and 5 females; age range: 20s–40s, mean age: 30.8 years, SD = 9.58 years). All participants were right-handed except for two left-handed participants. The mean completion time of all participants for all tasks was 88 minutes.

6.1 Experimental Conditions

In this study, we evaluated two conditions: posture and ring shape conditions. As the posture condition, we used the sighted and eyes-free condition as shown in Figure 10. In Study 2, we added an eyes-free condition in which participants operated the device without looking at it. Because eyes-free interaction enables users to perform other tasks without attending to the input device, it is considered useful in mobile and wearable settings[61, 64]; we therefore included this condition in our study.

Using the two posture conditions, we compared Flat and Beveled Rings to evaluate how ring shape affected the accuracy of touch gestures. Adding more conditions requires more frequent ring changes as well as additional instruction and practice for each condition, which increases participant burden. As Study 1 showed that Beveled Ring achieved the highest surface targeting accuracy on the flat middle surface among the three ring shapes. We excluded Rounded Ring in Study 2 to reduce participant burden and evaluated performance by comparing Beveled Ring with Flat Ring as a baseline. The ring width was set to 6 mm, as this width achieved the highest accuracy on the left and right edges under the beveled condition in Study 1. The factors were combined factorially to yield four conditions: Flat–Sighted, Flat–Eyes-free, Beveled–Sighted, and Beveled–Eyes-free.

6.2 Apparatus

We describe the apparatus used in Study 2, including the ring device, the capacitive sensing setup, and the ring's electrode layout.

6.2.1 Ring Device. The schematics of the rings used in the experiment are shown in Figure 1A. The ring bodies were newly 3D-printed from a flexible material, providing sufficient flexibility to fit individual finger sizes. Each ring had a thickness of 3 mm, a band width of 6 mm, and an inner diameter of 16 mm. In the beveled ring, a 1.5 mm, 45° chamfer was applied to each edge, resulting in a 3 mm-wide flat middle surface. To detect SwipeUp/Down on the left and right edges, the electrodes on each edge were split into upper and lower segments, with a 5 mm vertical gap between the upper and lower electrodes (measured edge-to-edge).

6.2.2 Capacitive Sensing. In Study 2, we used an MPR121 capacitive touch sensing module for touch detection to obtain more stable capacitance measurements from multiple electrodes. The module measures the capacitance of each electrode using the same self-capacitance sensing principle as in Study 1. We use the Adafruit MPR121 library in conducting the capacitive measurements. The



Figure 10: Posture conditions in Study 2: sighted and eyes-free conditions.

threshold for touch detection was determined following the same procedure used in Study 1. In Study 2, the touch thresholds of the MPR121 were set in the range 5–75 for the participants.

6.2.3 Electrode Layout. For the experimental ring device, we aimed to minimize the number of electrodes. Results of the Study 1 suggested that SwipeUp/Down on the middle was difficult to perform accurately. Therefore, this surface was designed to support only tap input, which is easier to execute than swiping. Consequently, we used a single-electrode configuration for the middle surface. To determine whether the single electrode on the middle surface should be placed in the upper, lower, or both regions, we conducted a preliminary study.

In the preliminary study, we evaluated tap gesture classification accuracy using a 6 mm Beveled Ring, configured as in Study 1, in which each electrode was divided into upper and lower parts. Following C1 (Figure 6B), we classified Touch-L/M/R separately for the upper and lower parts based on which electrode(s) were activated. A trial was judged valid only if exactly one part (upper or lower) and only the intended electrode (L/M/R) was activated; activating both parts was treated as an error. Ten participants performed Touch-L, Touch-M, and Touch-R tap gestures on the upper and lower parts of the Beveled Ring (i.e., six touch gestures) under both sighted and eyes-free conditions. Each participant completed one training session and ten experimental sessions per condition, with each session consisting of the six gestures performed once in randomized order. The resulting classification accuracy for top middle touch in the sighted and eyes-free conditions was 84.0% and 57.0%, respectively, whereas for bottom middle touches it was 94.0% and 84.0%, respectively. In the sighted condition, the accuracies at the other locations were all above 90%, and in the eyes-free condition, they were all above 80%. Specifically, accuracy for top middle touch was significantly lower than for bottom middle touch in the eyes-free condition, indicating that top middle touch yielded lower accuracy. Because the results showed low accuracy for top middle touch, we did not employ a top middle electrode in Study 2.

In summary, our experimental ring device used in this study employed five electrodes in total (Figure 1A): four on the left and right surfaces (upper and lower on each side) and one on the lower part of the middle surface. Flat Ring used as a baseline was configured with the same electrode layout.

6.3 Touch Gesture Set for Beveled Ring

In this study, we define a set of nine touch gestures (Figure 2) for a beveled ring device that uses its beveled surfaces to enable precise and expressive touch input. This set expands upon the five basic gestures that are typically performed on a single input surface (a tap and four directional swipes: up, down, left, and right) [17, 54] to include a total of nine gestures. We set the size of the gesture set to nine, corresponding to the upper bound of the most preferred range of the number of gestures (5–9) [13]. Specifically, by using three input surfaces (left, middle, and right), we extended the tap gesture into three variants yielded by taps on each surface. Based on the results of Study 1, the flat middle surface was used only for tap gestures, as tapping is simpler than swiping. Additionally, we enabled SwipeUp/Down gestures on both the left and right edges, expanding the two vertical swipe gestures previously available on a single input surface into four distinct gestures.

As a result, the gesture set supported a total of nine gestures: three Touch gestures (left, middle, and right), two horizontal swipe gestures (left and right), and four vertical swipe gestures (SwipeUp and SwipeDown on the left and right surfaces).

6.3.1 Gesture Classification Pattern. To classify the nine touch gestures (Figure 2) on ring devices, we designed a touch pattern based on touches on five electrodes and their temporal order. The valid pattern for each gesture is shown in Figure 11.

For Touch-L and Touch-R, touch with the middle electrode is optional (it may be touched or not). For Touch-M, touch with the middle electrode is required, and the left and right electrodes must not be touched. Alternatively, trials in which all three bottom electrodes are touched are classified only if the release time difference between the left and right electrodes was less than 80 ms.

For SwipeDown-L/R, first touch the top electrode on either the left or right side, then touch any bottom electrode. The gesture was classified if the bottom touch started at least 70 ms after the top touch. For SwipeUp-L/R, first touch any bottom electrode, then touch the top electrode on either the left or right side. The gesture is classified if the top touch started at least 70 ms after the bottom touch.

For Swipe-L/R, first touch an electrode on either the left or right side, and then touch the electrode on the opposite side. Because the finger may briefly lift off all electrodes during Swipe-L and Swipe-R gestures, we set a waiting time of 610 ms for gesture classification in our experimental device.

6.4 Tasks

Participants performed the nine touch gestures shown in Figure 2 under each condition. Each participant completed one training session and 16 experimental sessions per condition; in each session, the nine gestures were performed once each in randomized order. In total, we collected 6,912 gesture trials (12 participants × 2 ring shapes × 2 postures × 16 sessions × 9 gestures).

To control for order effects, we employed a Latin square design and assigned the 12 participants equally to four groups (three participants per group). Starting from a base sequence of the four

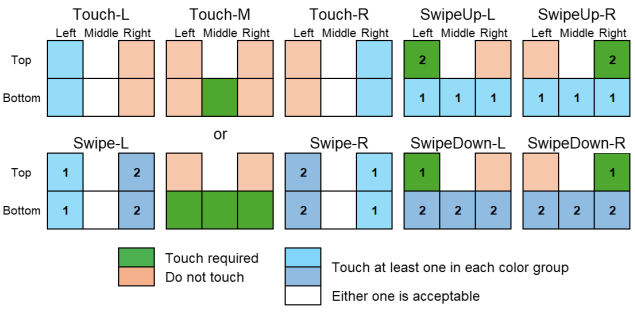


Figure 11: Nine touch gesture classification patterns. Gestures are classified from touch patterns on five electrodes arranged on the ring. Each cell corresponds to an electrode location. Numbers indicate touch order (1 → 2).

conditions (Flat-Sighted, Flat-Eyes-free, Beveled-Sighted, Beveled-Eyes-free), we rotated the starting position so that each group of participants began with a different condition. This ensured that all four conditions appeared equally often in each position in the sequence.

6.5 Procedure

The procedure largely followed Study 1. Each session began with donning the ring and receiving task instructions. We used two posture settings: sighted and eyes-free. In the eyes-free condition, a box was placed over the participant's hand so that the ring remained out of view during gesture performance; in the sighted condition, no box was used and participants were allowed to look at their hand. Participants then read a document describing the experimental procedure and the gesture set (Figure 2) and entered a practice phase. During the initial practice, real-time electrode signals were visualized as bar plots, and participants practiced each gesture while monitoring these values. After this, participants completed a practice session in which each gesture was performed once in randomized order. During the practice session, visual feedback regarding correctness (a circle or a cross) was shown after each trial. If the execution was correct, participants proceeded to the next gesture; otherwise, they repeated the gesture. If a correct execution could not be achieved after multiple trials, the gesture was skipped, and the next practice trial began. After the practice phase, participants completed 16 experimental sessions for each pattern. To minimize fatigue, the 16 sessions per condition were split into two equal blocks of eight sessions. After each block, participants removed the ring, took a break, and then put it back on before resuming the task. Participants rested for at least 30 s after the first block and at least 1 min after completing all 16 sessions in each condition.

6.6 Results

To evaluate the effects of ring shapes and postures, we analyzed touch gesture classification accuracy and false positive rate (FPR) for the nine touch gestures in each condition. Error trials were excluded from the analysis, and the remaining trial data were used.

Figure 12 shows the mean classification accuracy across participants. Under the sighted condition, accuracies were 63.8% (SD = 5.32%) for Flat Ring (Flat) and 92.9% (SD = 4.80%) for Beveled Ring (Bevel); under the eyes-free condition, accuracies were 62.9% (SD = 7.61%) and 91.8% (SD = 9.10%), respectively. The corresponding confusion matrices are shown in Figure 13. Figure 12 shows the mean FPRs across participants. Under the sighted condition, FPRs were 4.41% (SD = 0.62%) for Flat and 0.88% (SD = 0.59%) for Bevel; under the Eyes-free condition, they were 4.55% (SD = 1.00%) and 1.00% (SD = 1.13%), respectively.

For significance testing, we treated participants as a random factor, and ring shape (Flat and Bevel) and posture (sighted and eyes-free) as within-participant factors. Because the assumptions of normality and homogeneity were not satisfied, we conducted a Scheirer-Ray-Hare test on classification accuracies and FPRs, using the R package rcompanion. Post-hoc pairwise comparisons were then performed using the Wilcoxon signed-rank test with Bonferroni-adjusted p-values.

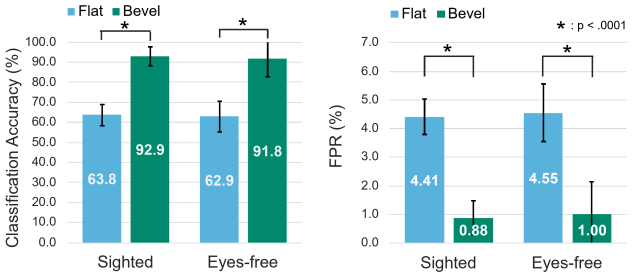


Figure 12: Mean classification accuracies and FPRs across participants in Study 2. Each bar means ± one SD between participants. Beveled Ring had a significantly higher classification accuracy and lower FPR than Flat Ring under both posture conditions.

The results showed there was a significant main effect of ring shape ($H(1) = 35.30\, p < .001$, $\eta^2 = 0.852$). The main effect of posture was not significant ($H(1) = 0.005$, $p = 0.942$, $\eta^2 = 0.002$), and the interaction was not significant ($H(1) = 0.018$, $p = 0.893$, $\eta^2 = 0.003$). We ran a Wilcoxon signed-rank test (Bonferroni), and the result showed that classification accuracy is significantly higher for Bevel (92.33%) than for Flat (63.36%) under both sighted and eyes-free conditions (sighted and eyes-free: $adj.p < .001$). The effect sizes (Cohen's d) for the comparisons between Flat and Bevel were 2.83 (sighted) and 3.45 (eyes-free).

For the FPRs, a Scheirer-Ray-Hare test showed a significant main effect of shape, with lower FPR for Bevel than Flat ($H(1) = 35.30$, $p < .001$, $\eta^2 = 0.751$). The main effect of posture ($H(1) = 0.034$, $p = 0.853$, $\eta^2 = 0.0007$) and the interaction ($H(1) = 0.002$, $p = 0.967$, $\eta^2 < 0.0001$) were not significant. Wilcoxon signed-rank test with Bonferroni adjustment confirmed that within each posture, Bevel had a significantly lower FPR than Flat under both sighted and eyes-free conditions (sighted and eyes-free: $adj.p < .001$). The effect sizes (Cohen's d) for the comparisons between Flat and Bevel were 2.90 (sighted) and 3.17 (eye-free).

6.6.1 Discussion. We analyze and discuss here the results of Study 2. As shown in Figure 13, confusion was observed in touch gesture classification on Flat Ring. First, Touch-L/R were frequently misclassified as Swipe-L/R gestures. This is presumed to result from accidental touches on the surface opposite the intended left/right touches, leading single taps to be misclassified as swipes (e.g., a left tap followed by a spurious right surface touch being labeled a Swipe-R). A similar misclassification was observed for the SwipeUp/Down gestures. We thought that accidental touches on the opposite side at the beginning or end of SwipeUp/Down gestures caused misclassification into Swipe-L/R.

On Flat Ring, left/right touch input often resulted in chattering-like contact on the opposite side, degrading the classification accuracy and increasing confusion between gesture sets. In contrast, Beveled Ring, consistent with the results of Study 1, allowed users to accurately distinguish between left and right surfaces. Consequently, it enabled higher-accuracy, lower-FPR classification of the nine gestures using accurately simple touch patterns and temporal ordering compared with Flat Ring.

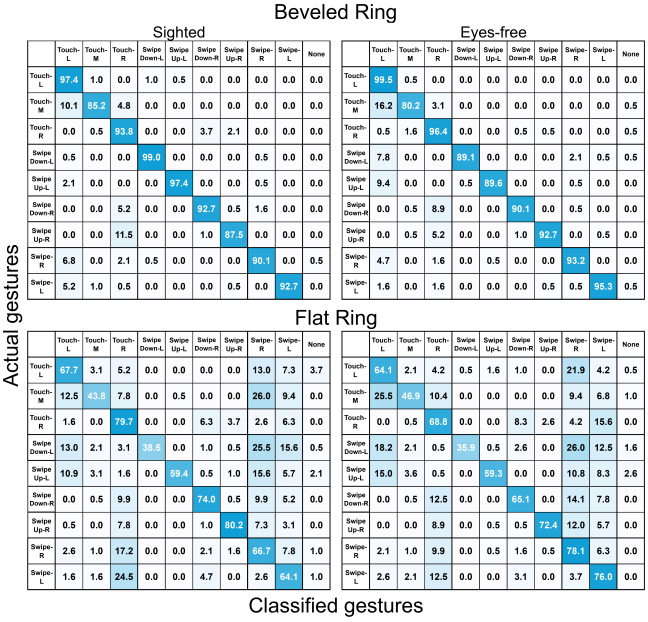


Figure 13: Confusion matrices of classification accuracy for ring and posture conditions in Study 2. Beveled Ring had a significantly higher classification accuracy than Flat Ring under both posture conditions.

Across both conditions, SwipeUp/Down gestures were sometimes confused with Touch gestures, and this confusion occurred more frequently in the sighted condition than in the eyes-free condition. We suspect that this occurred when the swipe distance was short, allowing participants to fail to reliably contact both the upper and lower electrodes, which resulted in the gesture being interpreted as a touch. These results suggest that an appropriate vertical spacing between the electrodes, at which such confusions are less likely, could further improve recognition accuracy. In addition, for Touch-M, we observed in both conditions a tendency for users to contact only the left or right side instead of the intended middle area, which also contributed to reduced classification accuracy.

In summary, Beveled Ring achieves significantly higher classification accuracy and lower false positive rate (FPR) compared to Flat Ring under both sighted and eyes-free conditions, achieving 92.9% and 91.8% accuracy in the sighted and eyes-free conditions, respectively, with FPR $\leq$ 1% (0.88% sighted; 1.00% eyes-free). This result suggests that ring shape design, such as beveled surfaces, can improve the touch input accuracy of touch gestures on ring devices with 6 mm band width.

7 Discussion

7.1 Ring Shape Effect on Touch Input Accuracy

7.1.1 Band Width and Ring Shape Effect on Surface Targeting Accuracy. Study 1 found that Flat Ring increased the difficulty of distinguishing left and right surface touches as ring width decreased. These findings suggest that measures to preserve left and right edge separability are necessary when designing edge touch interactions for even more miniaturized rings.

Moreover, the results showed that as band width decreases, Beveled and Rounded Rings have higher surface targeting accuracy than Flat Ring, indicating that ring shape facilitates improving touch input accuracy on the left and right edges in narrow ring devices. Under these conditions (4 mm and 6 mm), Beveled and Rounded Rings allow users to accurately perform two vertical swipes (SwipeUp/Down-L and SwipeUp/Down-R), whereas Flat Ring allows users to accurately perform only a single vertical swipe (SwipeUp/Down-M).

7.1.2 Ring Shapes Effect on Classification Accuracy of Touch Gestures. The results of Study 2 show that a 6 mm-wide Beveled Ring can achieve 92.9% (sighted) and 91.8% (eyes-free) classification accuracy with FPR $\leq$ 1% (0.88% sighted; 1.00% eyes-free) across nine touch gestures. The results also showed that Beveled Ring offers significantly better classification accuracy and FPRs than Flat Ring. These results suggest that beveled surfaces are promising for improving touch input accuracy on ring devices.

7.2 Real-World Factors and Practical Considerations

We discuss practical factors relevant to the real-world deployment of our method, including unintended activation, power consumption, and potential applications.

In daily use, unintended activations may occur due to finger-to-finger interference and other everyday hand movements. Because this work is an initial exploration, this issue was not addressed in sufficient depth. One possible solution to mitigate such unintended activations is to introduce an activation gesture that switches the device into a gesture-accepting mode. One possible activation gesture is a double-tap, which is also used on smartphones [45, 60]. Investigating appropriate activation mechanisms and their impact on usability is one direction for future work.

Power consumption is another important consideration for practical deployment. There are capacitive touch sensor ICs (e.g., Microchip CAP1005) that can continuously monitor the presence of touch while operating in a low-power mode, maintaining a standby current of only a few μA. By integrating such ICs, ring devices adopting our method could reduce power consumption while maintaining touch detection capability.

Our method provides precise and expressive ring touch inputs, such as two vertical swipes and three distinct touch gestures on three distinct surfaces, enabling subtle, eyes-free interaction. Our technique can be applied in contexts such as smart homes [7] and wearable devices, including smart glasses [52]. In these interactions, users invoke a variety of applications and functions, as well as adjust the parameters of these functions. For example, in a music application, two vertical swipes could be mapped to separate menus, enabling users to quickly switch tracks on one side while adjusting volume on the other. In a smart home scenario, one menu could be used for rapidly switching between smart devices (e.g., lights, speakers, air conditioners), while the other menu controls device-specific functions such as brightness, temperature, or mode selection. For smart glasses, one menu could provide global command shortcuts (e.g., back, home, application list), while the other

offers application-specific functions. Furthermore, assignment of the three tap gestures on each of three surfaces offers fine-grained adjustments of functions and selection. Swipe-L/R further allows the assignment of less frequently used yet useful functions, such as switching between categories (e.g., wearable devices and smart home control) or switching between open applications. We believe that our technique has the potential to support more flexible and expressive control while maintaining subtle, eyes-free interaction.

We introduced a wait time to distinguish between Touch gestures and Swipe-L/R because the finger may briefly lift off the electrodes during a swipe. The wait time was set to 610 ms. Using Study 2 data, we computed the required wait time for all trials correctly classified as Swipe-L/R, and this time covered approximately 95% of these trials. The maximum required wait time to cover 95% of these trials was 574.0 ms for Beveled Ring and 609.8 ms for Flat Ring (the larger of the two). In Study 2, participants were instructed to perform gestures as accurately as possible; therefore, the required wait time likely included a buffer (i.e., it may have been longer than necessary in practice). Consistent with this, the 80% and 50% required wait times were 433.6/445.0 ms and 305.0/223.0 ms, respectively, for Beveled and Flat Rings. Further investigation of the wait time required for different usage scenarios remains future work.

7.3 Beveled Design Effects

Similar to a rounded design, a beveled design eliminates sharp edges and is expected to minimize stress when fingers come into contact with the ring. Additionally, the beveled design results in a smaller cross-sectional volume than the rounded design used in this study, which suggests that it may reduce contact with adjacent fingers. Consequently, a beveled design may be less noticeable in terms of finger-ring contact and provide greater comfort than flat or rounded designs. However, future studies are needed to examine the extent to which wearing comfort is actually improved.

The beveled profile also affects the internal design of smart rings. In our prototype, the ring cross-section has a thickness of 3 mm with a 1.5 mm, 45° chamfer on both sides. Under this design, the effective inner height near the outer edges of the band is about 1–1.5 mm. Therefore, the internal layout should take this constraint into account, for example, by placing wiring and thin components near the outer periphery and locating taller ICs closer to the center of the ring.

7.4 Limitation

Although beveled surfaces show promise for achieving expressiveness and accuracy in touch input on ring devices, they have some limitations. In this study, we evaluated the effect of ring shape using a sparse electrode layout across the three input surfaces. Our evaluation suggests that the ring-shape design can improve input accuracy under our study conditions. However, it remains unclear whether this effect is consistent in ring devices that utilize dense electrode arrays, such as touch panels. This is a limitation of the current investigation. In this study, we used a simple rule-based classifier that incorporated touch patterns and their temporal order. In future work, we plan to investigate other classification approaches, including richer temporal modeling and relative signal-change features, which may further improve recognition accuracy.

Since our focus was on the effect of surface bveling, the experimental setup device uses external electronics instead of embedding the circuit within the ring. The next step is a self-contained ring device that integrates a microcontroller with capacitive touch sensing functions and ring electrodes, and a battery. There are flexible PCB assemblies for smart rings available as open source components [62]. We believe that by incorporating electrodes and a microcontroller with capacitive sensing capabilities into these assemblies, it is possible to create our ring device with embedded circuits.

In this study, the initial evaluation of the effect of ring shape on input accuracy was conducted under controlled conditions with the hand resting on a desk. Investigating other scenarios, such as walking or performing gestures with the arm lowered, would likely reveal additional attributes of our method. While such explorations could provide more comprehensive insights into the practical utility of our method, addressing them fully is beyond the scope of this initial exploration.

7.5 Implications

Unlike prior ring devices, our method leverages the ring shape itself as an input-enabling element. We evaluated the method with two simple touch gestures, touch and swipe, while prior work examined a broader repertoire of touch gestures (multi-touch [10, 40, 53], rolling [43], and double-taps [35]). Within this broader context, ring shape design has the potential to serve as one of the design principles that enables higher accuracy and finer-grained expressive touch input.

In terms of the development of touch input on rings, by focusing on the beveled surface, we have shown the potential for resolving the issues with touch input on rings and for improving input accuracy. We believe that this work shows a new research direction for ring device research, which has been dominated by technological interventions in sensing technologies.

8 Conclusion

We investigated how beveled surfaces, in addition to the flat outer surface, affect touch input on a ring device to enable expressive and accurate touch input. Our study results showed that with band widths of 6 mm or less, Flat Ring had low accuracy in distinguishing left and right edge touch due to fat finger effects. In contrast, Beveled and Rounded Rings achieved higher accuracy than Flat Rings at these narrow widths. We further evaluated the classification of nine touch gestures on a ring device, comparing it to Bevel and Flat Ring with a 6 mm band width. Beveled Ring achieved significantly higher classification accuracy and lower false positive rate (FPR) compared to Flat Ring under both sighted and eyes-free conditions. Given these results, we identify the potential of beveled surfaces as a promising method for expressive and precise touch input on a ring device. We hope this work lays a foundation for expanding touch input while preserving wearability, thus advancing ring devices toward more capable smart rings.

References

[1] Daniel Ashbrook, Patrick Baudisch, and Sean White. 2011. Nenya: Subtle and Eyes-Free Mobile Input with a Magnetically-Tracked Finger Ring. In *Proceedings of the SIGCHI Conference on Human Factors in Computing Systems* (Vancouver,

BC, Canada) *(CHI '11)*. Association for Computing Machinery, New York, NY, USA, 2043–2046. doi:10.1145/1978942.1979238

[2] Myroslav Bachynskyi, Gregorio Palmas, Antti Oulasvirta, Jürgen Steimle, and Tino Weinkauf. 2015. Performance and Ergonomics of Touch Surfaces: A Comparative Study using Biomechanical Simulation. In *Proceedings of the 33rd Annual ACM Conference on Human Factors in Computing Systems* (Seoul, Republic of Korea) *(CHI '15)*. Association for Computing Machinery, New York, NY, USA, 1817–1826. doi:10.1145/2702123.2702607

[3] Paul Bagder and Paul Stoffregen. 2016. CapacitiveSensor Library. https://docs.arduino.cc/libraries/capacitivesensor/. Accessed: 2025-09-11.

[4] Patrick Baudisch and Gerry Chu. 2009. Back-of-Device Interaction Allows Creating Very Small Touch Devices. In *Proceedings of the SIGCHI Conference on Human Factors in Computing Systems* (Boston, MA, USA) *(CHI '09)*. Association for Computing Machinery, New York, NY, USA, 1923–1932. doi:10.1145/1518701.1518995

[5] Rahul Bhaumik, Kevin F Mwaita, Fabio Solaroli, Aftab Ahmed, Antonella De Angeli, and Michael Haller. 2024. Interaction with a 3D Surface for an Innovative Input Experience on a Central Console. In *Proceedings of the 16th International Conference on Automotive User Interfaces and Interactive Vehicular Applications* (Stanford, CA, USA) *(AutomotiveUI '24)*. Association for Computing Machinery, New York, NY, USA, 136–148. doi:10.1145/3640792.3675707

[6] Laura-Bianca Bilius and Radu-Daniel Vatavu. 2023. "I Could Wear It All of the Time, Just Like My Wedding Ring:" Insights into Older People's Perceptions of Smart Rings. In *Extended Abstracts of the 2023 CHI Conference on Human Factors in Computing Systems* (Hamburg, Germany) *(CHI EA '23)*. Association for Computing Machinery, New York, NY, USA, Article 165, 8 pages. doi:10.1145/3544549.3585771

[7] Runze Cai, Nuwan Nanayakkarawasam Peru Kandage Janaka, Shengdong Zhao, and Minghui Sun. 2023. ParaGlassMenu: Towards Social-Friendly Subtle Interactions in Conversations. In *Proceedings of the 2023 CHI Conference on Human Factors in Computing Systems* (Hamburg, Germany) *(CHI '23)*. Association for Computing Machinery, New York, NY, USA, Article 721, 21 pages. doi:10.1145/3544548.3581065

[8] Taylor & Francis Knowledge Centers. 2025. Chamfers – Knowledge and References. https://taylorandfrancis.com/knowledge/Engineering_and_technology/Engineering_support_and_special_topics/Chamfers/ Accessed: 2025-12-03.

[9] Xiang 'Anthony' Chen, Julia Schwarz, Chris Harrison, Jennifer Mankoff, and Scott E. Hudson. 2014. Air+Touch: Interweaving Touch & In-Air Gestures. In *Proceedings of the 27th Annual ACM Symposium on User Interface Software and Technology* (Honolulu, Hawaii, USA) *(UIST '14)*. Association for Computing Machinery, New York, NY, USA, 519–525. doi:10.1145/2642918.2647392

[10] Mauricio Cirelli and Ricardo Nakamura. 2014. A Survey on Multi-touch Gesture Recognition and Multi-touch Frameworks. In *Proceedings of the Ninth ACM International Conference on Interactive Tabletops and Surfaces* (Dresden, Germany) *(ITS '14)*. Association for Computing Machinery, New York, NY, USA, 35–44. doi:10.1145/2669485.2669509

[11] Tilman Dingler, Rufat Rzayev, Alireza Sahami Shirazi, and Niels Henze. 2018. Designing Consistent Gestures Across Device Types: Eliciting RSVP Controls for Phone, Watch, and Glasses. In *Proceedings of the 2018 CHI Conference on Human Factors in Computing Systems* (Montreal QC, Canada) *(CHI '18)*. Association for Computing Machinery, New York, NY, USA, 1–12. doi:10.1145/3173574.3173993

[12] Ken Hinckley, Seongkook Heo, Michel Pahud, Christian Holz, Hrvoje Benko, Abigail Sellen, Richard Banks, Kenton O'Hara, Gavin Smyth, and William Buxton. 2016. Pre-Touch Sensing for Mobile Interaction. In *Proceedings of the 2016 CHI Conference on Human Factors in Computing Systems* (San Jose, California, USA) *(CHI '16)*. Association for Computing Machinery, New York, NY, USA, 2869–2881. doi:10.1145/2858036.2858095

[13] Masoumehsadat Hosseini, Heiko Mueller, and Susanne Boll. 2024. Controlling the Rooms: How People Prefer Using Gestures to Control Their Smart Homes. In *Proceedings of the 2024 CHI Conference on Human Factors in Computing Systems* (Honolulu, HI, USA) *(CHI '24)*. Association for Computing Machinery, New York, NY, USA, Article 550, 18 pages. doi:10.1145/3613904.3642687

[14] Han Huang, Tingyu Cheng, Jinzhi Ye, Yuhui Zhao, Yiyang Wang, Haiqing Xu, Abigale Stangl, and HyunJoo Oh. 2025. Eliciting Design Guidelines of Paper-Based Tactile Interfaces for Eyes-Free Scenarios. In *Proceedings of the Nineteenth International Conference on Tangible, Embedded, and Embodied Interaction (TEI '25)*. Association for Computing Machinery, New York, NY, USA, Article 12, 15 pages. doi:10.1145/3689050.3704930

[15] Mohit Jain and Ravin Balakrishnan. 2012. User Learning and Performance with Bezel Menus. In *Proceedings of the SIGCHI Conference on Human Factors in Computing Systems* (Austin, Texas, USA) *(CHI '12)*. Association for Computing Machinery, New York, NY, USA, 2221–2230. doi:10.1145/2207676.2208376

[16] Shaun K. Kane, Meredith Ringel Morris, and Jacob O. Wobbrock. 2013. Touchplates: Low-Cost Tactile Overlays for Visually Impaired Touch Screen Users. In *Proceedings of the 15th International ACM SIGACCESS Conference on Computers and Accessibility* (Bellevue, Washington) *(ASSETS '13)*. Association for Computing Machinery, New York, NY, USA, Article 22, 8 pages. doi:10.1145/2513383.2513442

[17] Hsin-Liu (Cindy) Kao, Artem Dementyev, Joseph A. Paradiso, and Chris Schmandt. 2015. NailO: Fingernails as an Input Surface. In *Proceedings of the 33rd Annual ACM Conference on Human Factors in Computing Systems* (Seoul, Republic of Korea) *(CHI '15)*. Association for Computing Machinery, New York, NY, USA, 3015–3018. doi:10.1145/2702123.2702572

[18] Junhyeok Kim, William Delamare, and Pourang Irani. 2018. ThumbText: Text Entry for Wearable Devices Using a Miniature Ring. In *Proceedings of the 44th Graphics Interface Conference* (Toronto, Canada) *(GI '18)*. Canadian Human-Computer Communications Society, Waterloo, CAN, 18–25. doi:10.20380/GI2018.04

[19] Jiwan Kim, Mingyu Han, and Ian Oakley. 2025. BudsID: Mobile-Ready and Expressive Finger Identification Input for Earbuds. In *Proceedings of the 2025 CHI Conference on Human Factors in Computing Systems (CHI '25)*. Association for Computing Machinery, New York, NY, USA, Article 347, 17 pages. doi:10.1145/3706598.3714133

[20] Yuki Kubo, Buntarou Shizuki, and Jiro Tanaka. 2016. B2B-Swipe: Swipe Gesture for Rectangular Smartwatches from a Bezel to a Bezel. In *Proceedings of the CHI Conference on Human Factors in Computing Systems* (San Jose, California, USA) *(CHI '16)*. Association for Computing Machinery, New York, NY, USA, 3852–3856. doi:10.1145/2858036.2858216

[21] Elina Kuosmanen, Aku Visuri, Saba Kheirinejad, Niels van Berkel, Heli Koskimäki, Denzil Ferreira, and Simo Hosio. 2022. How Does Sleep Tracking Influence Your Life? Experiences from a Longitudinal Field Study with a Wearable Ring. *Proceedings of the ACM on Human-Computer Interaction* 6, MHCI, Article 185 (Sept. 2022), 19 pages. doi:10.1145/3546720

[22] Benjamin Lafreniere, Carl Gutwin, Andy Cockburn, and Tovi Grossman. 2016. Faster Command Selection on Touchscreen Watches. In *Proceedings of the 2016 CHI Conference on Human Factors in Computing Systems* (San Jose, California, USA) *(CHI '16)*. Association for Computing Machinery, New York, NY, USA, 4663–4674. doi:10.1145/2858036.2858166

[23] Tuomas Lappalainen, Lasse Virtanen, and Jonna Häkkilä. 2016. Experiences with Wellness Ring and Bracelet Form Factor. In *Proceedings of the 15th International Conference on Mobile and Ubiquitous Multimedia* (Rovaniemi, Finland) *(MUM '16)*. Association for Computing Machinery, New York, NY, USA, 351–353. doi:10.1145/3012709.3016065

[24] Gierad Laput, Eric Brockmeyer, Scott E. Hudson, and Chris Harrison. 2015. Acoustruments: Passive, Acoustically-Driven, Interactive Controls for Handheld Devices. In *Proceedings of the 33rd Annual ACM Conference on Human Factors in Computing Systems* (Seoul, Republic of Korea) *(CHI '15)*. Association for Computing Machinery, New York, NY, USA, 2161–2170. doi:10.1145/2702123.2702414

[25] Huy Viet Le, Sven Mayer, and Niels Henze. 2018. InfiniTouch: Finger-Aware Interaction on Fully Touch Sensitive Smartphones. In *Proceedings of the 31st Annual ACM Symposium on User Interface Software and Technology* (Berlin, Germany) *(UIST '18)*. Association for Computing Machinery, New York, NY, USA, 779–792. doi:10.1145/3242587.3242605

[26] Oura Health Ltd. 2024. Oura Ring 4. https://ouraring.com/product/rings/oura-ring-4/black Accessed: 2025-09-11.

[27] Amit Magdum, E. Sivaraman, and Prasad B. Honnavalli. 2021. Contactless Transaction Using Wearable Ring with Biometric Fingerprint Security Feature. In *Computer Networks and Inventive Communication Technologies*, S. Smys, Ram Palanisamy, Álvaro Rocha, and Grigorios N. Beligiannis (Eds.). Springer Nature Singapore, Singapore, 653–666.

[28] Michele Magno, Giovanni A. Salvatore, Petar Jokic, and Luca Benini. 2019. Self-Sustainable Smart Ring for Long-Term Monitoring of Blood Oxygenation. *IEEE Access* 7 (2019), 115400–115408. doi:10.1109/ACCESS.2019.2928055

[29] Sven Mayer, Huy Viet Le, and Niels Henze. 2018. Designing finger orientation input for mobile touchscreens. In *Proceedings of the 20th International Conference on Human-Computer Interaction with Mobile Devices and Services* (Barcelona, Spain) *(MobileHCI '18)*. Association for Computing Machinery, New York, NY, USA, Article 29, 9 pages. doi:10.1145/3229434.3229444

[30] Cameron S. Miner, Denise M. Chan, and Christopher Campbell. 2001. Digital Jewelry: Wearable Technology for Everyday Life. In *CHI '01 Extended Abstracts on Human Factors in Computing Systems* (Seattle, Washington) *(CHI EA '01)*. Association for Computing Machinery, New York, NY, USA, 45–46. doi:10.1145/634067.634098

[31] Ken Morling and Stéphane Danjou. 2022. *Geometric and Engineering Drawing* (4th ed.). Routledge, Chapter 7. doi:10.1201/9781003001386

[32] Suranga Nanayakkara, Roy Shilkrot, Kian Peen Yeo, and Pattie Maes. 2013. EyeRing: A Finger-Worn Input Device for Seamless Interactions with our Surroundings. In *Proceedings of the 4th Augmented Human International Conference* (Stuttgart, Germany) *(AH '13)*. Association for Computing Machinery, New York, NY, USA, 13–20. doi:10.1145/2459236.2459240

[33] Oliver Nowak, René Schäfer, Anke Brocker, Philipp Wacker, and Jan Borchers. 2022. Shaping Textile Sliders: An Evaluation of Form Factors and Tick Marks for Textile Sliders. In *Proceedings of the 2022 CHI Conference on Human Factors in Computing Systems* (New Orleans, LA, USA) *(CHI '22)*. Association for Computing Machinery, New York, NY, USA, Article 214, 14 pages. doi:10.1145/3491102.3517473

[34] Ian Oakley and Doyoung Lee. 2014. Interaction on the Edge: Offset Sensing for Small Devices. In *Proceedings of the SIGCHI Conference on Human Factors in Computing Systems* (Toronto, Ontario, Canada) *(CHI '14)*. Association for Computing

Machinery, New York, NY, USA, 169–178. doi:10.1145/2556288.2557138

[35] Ian Oakley, DoYoung Lee, MD. Rasel Islam, and Augusto Esteves. 2015. Beats: Tapping Gestures for Smart Watches. In *Proceedings of the 33rd Annual ACM Conference on Human Factors in Computing Systems* (Seoul, Republic of Korea) *(CHI '15)*. Association for Computing Machinery, New York, NY, USA, 1237–1246. doi:10.1145/2702123.2702226

[36] Makoto Ono, Buntarou Shizuki, and Jiro Tanaka. 2013. Touch & Activate: Adding Interactivity to Existing Objects using Active Acoustic Sensing. In *Proceedings of the 26th Annual ACM Symposium on User Interface Software and Technology* (St. Andrews, Scotland, United Kingdom) *(UIST '13)*. Association for Computing Machinery, New York, NY, USA, 31–40. doi:10.1145/2501988.2501989

[37] Pekka Parhi, Amy K. Karlson, and Benjamin B. Bederson. 2006. Target Size Study for One-Handed Thumb Use on Small Touchscreen Devices. In *Proceedings of the 8th Conference on Human-Computer Interaction with Mobile Devices and Services* (Helsinki, Finland) *(MobileHCI '06)*. Association for Computing Machinery, New York, NY, USA, 203–210. doi:10.1145/1152215.1152260

[38] Juho Rantakari, Virve Inget, Ashley Colley, and Jonna Häkkilä. 2016. Charting Design Preferences on Wellness Wearables. In *Proceedings of the 7th Augmented Human International Conference 2016* (Geneva, Switzerland) *(AH '16)*. Association for Computing Machinery, New York, NY, USA, Article 28, 4 pages. doi:10.1145/2875194.2875231

[39] Inka Rantala, Ashley Colley, and Jonna Häkkilä. 2018. Smart Jewelry: Augmenting Traditional Wearable Self-Expression Displays. In *Proceedings of the 7th ACM International Symposium on Pervasive Displays* (Munich, Germany) *(PerDis '18)*. Association for Computing Machinery, New York, NY, USA, Article 22, 8 pages. doi:10.1145/3205873.3205891

[40] Jun Rekimoto. 2002. SmartSkin: An Infrastructure for Freehand Manipulation on Interactive Surfaces. In *Proceedings of the SIGCHI Conference on Human Factors in Computing Systems* (Minneapolis, Minnesota, USA) *(CHI '02)*. Association for Computing Machinery, New York, NY, USA, 113–120. doi:10.1145/503376.503397

[41] RingConn LLC. 2025. RingConn Gen 2. https://ringconn.com/ Accessed: 2025-12-03.

[42] Volker Roth and Thea Turner. 2009. Bezel Swipe: Conflict-Free Scrolling and Multiple Selection on Mobile Touch Screen Devices. In *Proceedings of the SIGCHI Conference on Human Factors in Computing Systems* (Boston, MA, USA) *(CHI '09)*. Association for Computing Machinery, New York, NY, USA, 1523–1526. doi:10.1145/1518701.1518933

[43] Anne Roudaut, Eric Lecolinet, and Yves Guiard. 2009. MicroRolls: Expanding Touch-Screen Input Vocabulary by Distinguishing Rolls vs. Slides of the Thumb. In *Proceedings of the SIGCHI Conference on Human Factors in Computing Systems* (Boston, MA, USA) *(CHI '09)*. Association for Computing Machinery, New York, NY, USA, 927–936. doi:10.1145/1518701.1518843

[44] Anne Roudaut, Henning Pohl, and Patrick Baudisch. 2011. Touch Input on Curved Surfaces. In *Proceedings of the SIGCHI Conference on Human Factors in Computing Systems* (Vancouver, BC, Canada) *(CHI '11)*. Association for Computing Machinery, New York, NY, USA, 1011–1020. doi:10.1145/1978942.1979094

[45] Samsung Electronics Co., Ltd. 2025. Enable Double Tap to Turn off on my Galaxy Device. https://www.samsung.com/au/support/mobile-devices/enable-double-tap-to-turn-off/ Accessed: 2025-12-03.

[46] Samsung Electronics Co., Ltd. 2025. Galaxy Ring. https://www.samsung.com/us/rings/galaxy-ring/buy/galaxy-ring-size-10-titanium-silver-sm-q500nzsaxar/ Accessed: 2025-12-03.

[47] Shardul Sapkota, Ashwin Ram, and Shengdong Zhao. 2021. Ubiquitous Interactions for Heads-Up Computing: Understanding Users' Preferences for Subtle Interaction Techniques in Everyday Settings. In *Proceedings of the 23rd International Conference on Mobile Human-Computer Interaction* (Toulouse & Virtual, France) *(MobileHCI '21)*. Association for Computing Machinery, New York, NY, USA, Article 36, 15 pages. doi:10.1145/3447526.3472035

[48] Dominik Schürmann, Sergej Dechand, and Lars Wolf. 2017. OpenKeychain: An Architecture for Cryptography with Smart Cards and NFC Rings on Android. *Proc. ACM Interact. Mob. Wearable Ubiquitous Technol.* 1, 3, Article 99 (Sept. 2017), 24 pages. doi:10.1145/3130964

[49] Sougata Sen and David Kotz. 2020. VibeRing: Using Vibrations from A Smart Ring as An Out-of-band Channel for Sharing Secret Keys. In *Proceedings of the 10th International Conference on the Internet of Things* (Malmö, Sweden) *(IoT '20)*. Association for Computing Machinery, New York, NY, USA, Article 13, 8 pages. doi:10.1145/3410992.3410995

[50] Marcos Serrano, Eric Lecolinet, and Yves Guiard. 2013. Bezel-Tap Gestures: Quick Activation of Commands from Sleep Mode on Tablets. In *Proceedings of the SIGCHI Conference on Human Factors in Computing Systems* (Paris, France) *(CHI '13)*. Association for Computing Machinery, New York, NY, USA, 3027–3036. doi:10.1145/2470654.2481421

[51] Katie A. Siek, Yvonne Rogers, and Kay H. Connelly. 2005. Fat Finger Worries: How Older and Younger Users Physically Interact with PDAs. In *Proceedings of the 2005 IFIP TC13 International Conference on Human-Computer Interaction* (Rome, Italy) *(INTERACT'05)*. Springer-Verlag, Berlin, Heidelberg, 267–280. doi:10.1007/11555261_24

[52] Radu-Daniel Vatavu and Jean Vanderdonckt. 2020. Design Space and Users' Preferences for Smartglasses Graphical Menus: A Vignette Study. In *Proceedings of the 19th International Conference on Mobile and Ubiquitous Multimedia* (Essen, Germany) *(MUM '20)*. Association for Computing Machinery, New York, NY, USA, 1–12. doi:10.1145/3428361.3428467

[53] Nicolas Villar, Shahram Izadi, Dan Rosenfeld, Hrvoje Benko, John Helmes, Jonathan Westhues, Steve Hodges, Eyal Ofek, Alex Butler, Xiang Cao, and Billy Chen. 2009. Mouse 2.0: Multi-touch Meets the Mouse. In *Proceedings of the 22nd Annual ACM Symposium on User Interface Software and Technology* (Victoria, BC, Canada) *(UIST '09)*. Association for Computing Machinery, New York, NY, USA, 33–42. doi:10.1145/1622176.1622184

[54] Bryan Wang and Tovi Grossman. 2020. BlyncSync: Enabling Multimodal Smartwatch Gestures with Synchronous Touch and Blink. In *Proceedings of the 2020 CHI Conference on Human Factors in Computing Systems* (Honolulu, HI, USA) *(CHI '20)*. Association for Computing Machinery, New York, NY, USA, 1–14. doi:10.1145/3313831.3376132

[55] Ruolin Wang, Chun Yu, Xing-Dong Yang, Weijie He, and Yuanchun Shi. 2019. EarTouch: Facilitating Smartphone Use for Visually Impaired People in Mobile and Public Scenarios. In *Proceedings of the 2019 CHI Conference on Human Factors in Computing Systems* (Glasgow, Scotland Uk) *(CHI '19)*. Association for Computing Machinery, New York, NY, USA, 1–13. doi:10.1145/3290605.3300254

[56] Johann Wentzel, Greg d'Eon, and Daniel Vogel. 2020. Improving Virtual Reality Ergonomics Through Reach-Bounded Non-Linear Input Amplification. In *Proceedings of the 2020 CHI Conference on Human Factors in Computing Systems* (Honolulu, HI, USA) *(CHI '20)*. Association for Computing Machinery, New York, NY, USA, 1–12. doi:10.1145/3313831.3376687

[57] Daniel Wigdor, Clifton Forlines, Patrick Baudisch, John Barnwell, and Chia Shen. 2007. LucidTouch: A See-Through Mobile Device. In *Proceedings of the 20th Annual ACM Symposium on User Interface Software and Technology* (Newport, Rhode Island, USA) *(UIST '07)*. Association for Computing Machinery, New York, NY, USA, 269–278. doi:10.1145/1294211.1294259

[58] Jacob O. Wobbrock, Brad A. Myers, and John A. Kembel. 2003. EdgeWrite: A Stylus-Based Text Entry Method Designed for High Accuracy and Stability of Motion. In *Proceedings of the 16th Annual ACM Symposium on User Interface Software and Technology* (Vancouver, Canada) *(UIST '03)*. Association for Computing Machinery, New York, NY, USA, 61–70. doi:10.1145/964696.964703

[59] Pui Chung Wong, Kening Zhu, Xing-Dong Yang, and Hongbo Fu. 2020. Exploring Eyes-free Bezel-initiated Swipe on Round Smartwatches. In *Proceedings of the 2020 CHI Conference on Human Factors in Computing Systems* (Honolulu, HI, USA) *(CHI '20)*. Association for Computing Machinery, New York, NY, USA, 1–11. doi:10.1145/3313831.3376393

[60] Xiaomi Corporation. 2025. Xiaomi 15 FAQ. https://www.mi.com/global/support/faq/details/KA-541784/ Accessed: 2025-12-03.

[61] Bo Yi, Xiang Cao, Morten Fjeld, and Shengdong Zhao. 2012. Exploring User Motivations for Eyes-free Interaction on Mobile Devices. In *Proceedings of the SIGCHI Conference on Human Factors in Computing Systems* (Austin, Texas, USA) *(CHI '12)*. Association for Computing Machinery, New York, NY, USA, 2789–2792. doi:10.1145/2207676.2208678

[62] Hao Zhou, Taiting Lu, Yilin Liu, Shijia Zhang, Runze Liu, and Mahanth Gowda. 2023. One Ring to Rule Them All: An Open Source Smartring Platform for Finger Motion Analytics and Healthcare Applications. In *Proceedings of the 8th ACM/IEEE Conference on Internet of Things Design and Implementation* (San Antonio, TX, USA) *(IoTDI '23)*. Association for Computing Machinery, New York, NY, USA, 27–38. doi:10.1145/3576842.3582382

[63] Guanzhou Zhu, Dong Zhao, Yixuan Song, Zilong Wang, Anfu Zhou, Huadong Ma, Xiangbin Meng, Jingjia Wang, Chunli Shao, and Yida Tang. 2025. RingBP: Towards Continuous, Comfortable, and Generalized Blood Pressure Monitoring Using a Smart Ring. *Proceedings of the ACM on Interactive, Mobile, Wearable and Ubiquitous Technologies* 9, 2, Article 65 (June 2025), 24 pages. doi:10.1145/3731600

[64] Suwen Zhu, Jingjie Zheng, Shumin Zhai, and Xiaojun Bi. 2019. i'sFree: Eyes-Free Gesture Typing via a Touch-Enabled Remote Control. In *Proceedings of the 2019 CHI Conference on Human Factors in Computing Systems* (Glasgow, Scotland Uk) *(CHI '19)*. Association for Computing Machinery, New York, NY, USA, 1–12. doi:10.1145/3290605.3300678